

## NANOSIZED Ni/Pd CATALYSTS FOR OZONE DECOMPOSITION PREPARED BY EXTRACTIVE-PYROLYTIC METHOD

Todor Batakliiev<sup>1</sup>, Vladimir Georgiev<sup>1</sup>, Vladimir Blaskov<sup>3</sup>, Irina Stambolova<sup>3</sup>,

Yordanka Karakirova<sup>1</sup>, Vera Serga<sup>2</sup>, Slavcho Rakovsky<sup>1</sup>

<sup>1</sup> Institute of Catalysis, Bulgarian Academy of Sciences  
"Acad. G. Bonchev" Str., Bld. 11, 1113 Sofia, Bulgaria  
E-mail: [todor@ic.bas.bg](mailto:todor@ic.bas.bg)

Received 16 November 2015

Accepted 28 April 2016

<sup>2</sup> Riga Technical University  
Institute of Inorganic Chemistry  
Riga 2169, Latvia

<sup>3</sup> Institute of Inorganic Chemistry  
Bulgarian Academy of Sciences  
"Acad. G. Bonchev" Str., Bld. 11, 1113 Sofia, Bulgaria

---

### ABSTRACT

A range of catalytic samples made by extractive-pyrolytic method (EPM) and based on nickel and palladium nanoparticles supported on inorganic supports such as activated carbon, silica, alumina and aluminium hydroxide oxide were tested in the reaction of ozone decomposition. Aluminum oxides and oxyhydroxides occur in numerous crystallographic forms which exhibit different surface properties. The properties of the catalysts were confirmed by using various characterization techniques as BET, XRD, EPR and TEM. The EPM method allows small amounts of noble metals with particle size ranging from several nanometers to several tens of nanometers to be affixed onto the surface of the support. It was found that all treated Ni/Pd catalytic samples were active in the ozone decomposition reaction but the maximum conversion degree (more than 90 %) was achieved using aluminium hydroxide oxide-supported Ni/Pd system.

*Keywords:* ozone, decomposition, EPM, nanoparticles, EPR.

---

### INTRODUCTION

Ozone is widely used in the industrial and environmental processes such as semiconductor manufacturing, deodorization, disinfection and water treatment [1]. The residual ozone must be removed because it is an air contaminant on the ground level [2]. The heterogeneous catalytic decomposition [3] is an effective method for purification of waste gases containing ozone. The effect of different combinations of Fe, Ni, Ag, Co and Mn supported on zeolites has been investigated in ozone-assisted catalytic reaction for toluene removal [4]. Transition metal oxides as NiO/Al<sub>2</sub>O<sub>3</sub>, CoO/Al<sub>2</sub>O<sub>3</sub>, MnO<sub>2</sub>/Al<sub>2</sub>O<sub>3</sub>, Fe<sub>2</sub>O<sub>3</sub>/Al<sub>2</sub>O<sub>3</sub> and CuO/Al<sub>2</sub>O<sub>3</sub> prepared by

wetness impregnation also have been evaluated for the catalytic ozonation of toluene at room temperature. The NiO/Al<sub>2</sub>O<sub>3</sub>, CoO/Al<sub>2</sub>O<sub>3</sub> and MnO<sub>2</sub>/Al<sub>2</sub>O<sub>3</sub> have showed a higher efficiency for ozone and toluene decomposition [5]. The influence of nickel oxide addition on the activity of cement containing catalyst for ozone decomposition has been studied in ref. [6]. It is found that the addition of nickel oxide to the catalyst composition improves its catalytic properties. A decrease of the catalyst activity has been found upon decomposition of wet ozone. There is evidence that the presence of either activated carbon or Ni/AC improves considerably TOC removal during catalytic *p*-CBA ozonation. It has been found that *p*-CBA mineralization proceeds to a greater extent in the pres-

ence of Ni/AC catalyst instead of pure activated carbon as catalyst in the course of ozonation [7]. In another solid phase catalytic ozonation process aiming destruction of *p*-CBA as a model pollutant [8] titanium dioxide, cobalt oxide, nickel oxide, copper oxide, and a mixed metal oxide containing copper, zinc, and aluminium oxides have not accelerated the removal *p*-CBA in deionized water. However, cobalt oxide and the mixed metal oxide catalyst have been effective in accelerating the removal of *p*-CBA in a natural water matrix. An alumina-supported nickel oxide system has been found to be active in ozone decomposition at temperatures below 228 K [9]. Palladium catalysts have been used in catalytic ozonation for total oxidation of naphthalene [10], total oxidation of toluene [11] as well as in examination of the effect of calcinations temperature on the activity of Pd–Mn/SiO<sub>2</sub>–Al<sub>2</sub>O<sub>3</sub> catalysts in the reaction of ozone decomposition [12].

## EXPERIMENTAL

The extractive-pyrolytic method (EPM) was used for catalysts preparation. This simple and low cost method was described in our previous paper [13]. It allows small amounts of noble metals of particle size ranging from several nanometers to several tens of nanometers to be affixed onto the surface of the support. The inorganic supports were purchased from Aldrich. The organic precursors (the extracts) were prepared by extracting palladium and nickel from HCl solutions using 1 M *n*-trioctylamine (C<sub>8</sub>H<sub>17</sub>)<sub>3</sub>N solution in toluene. Different volumes of the extracts were used to impregnate the metals in order to obtain catalysts of different palladium and nickel contents. After impregnation, the toluene was evaporated by drying at 90°C - 110°C. Finally, the samples were heated up to 300°C at a rate of 10°C min<sup>-1</sup>. Thus the catalytic supports were loaded with 4.7 mass % of nickel and 0.17 mass % of palladium. The catalysts were denoted as 0.17Pd4.7Ni/SiO<sub>2</sub>, 0.17Pd4.7Ni/Al(OH)O, 0.17Pd4.7Ni/Al<sub>2</sub>O<sub>3</sub> and 0.17Pd4.7Ni/Carbon.

The ozone conversion degree measurements were carried out in a tubular glass reactor (6 mm × 150 mm) charged with 0.05 g - 0.06 g of catalyst bed. The experiments were performed at feed flow rates of 6.0 l h<sup>-1</sup> and inlet ozone concentration of 15 000 ppm. The ozone was generated by passing dry oxygen through a high-voltage silent-discharge ozone generator. The inlet and outlet

ozone concentrations were monitored using a BMT 964 UV absorption-type ozone analyzer.

X-ray powder diffraction patterns were recorded on a Bruker D8 advance powder diffractometer with Cu K $\alpha$  radiation source and SolX detector. The samples were scanned at 2 $\theta$  angles from 10° to 80° at a rate of 0.04° s<sup>-1</sup>. The X-ray intensity was operated with a current of 40 mA and a voltage of 45 kV.

The EPR spectra in the X-band were recorded as a first derivative of the absorption signal of a JEOL JES-FA 100 EPR spectrometer at room temperature. The samples were placed in special quartz tubes and were fixed at the centre of a standard TE<sub>011</sub> cylindrical resonator. The EPR spectra were recorded at modulation frequency of 100 kHz, microwave power of 1 mW, modulation amplitude of 0.5 mT, sweep of 500 mT, time constant of 0.3 s and sweep time of 2 min.

The microstructure of the catalyst was observed using a high-resolution transmission electron microscope (HRTEM JEOL 2100).

The specific surface area of the catalysts was measured by N<sub>2</sub> adsorption–desorption isotherms at 77 K using single point BET method in a FlowSorb 2300 instrument (Micromeritics Instrument Corporation).

## RESULTS AND DISCUSSION

The catalytic activity of the supported Ni/Pd catalysts in ozone decomposition was measured by monitoring the inlet and outlet ozone concentrations and calculating the conversion of ozone to molecular oxygen. It was found that all treated Ni/Pd catalytic samples have activity in respect to the ozone decomposition reaction but the maximum conversion degree (more than 90%) is observed in case of boehmite-supported Ni/Pd system (Fig. 1). This fact is probably due to the adsorption and desorption characteristics of aluminum oxide hydroxide as a support of Ni/Pd bimetallic catalyst. Ozone is easily adsorbed onto aluminum oxide hydroxide comparing to the other supports, because of the hydroxyl groups. The high conversion degree indicates that the hydroxyl groups of aluminum oxide hydroxide have excellent adsorption properties for ozone, the catalytic cycle of the process is steady and the catalyst prepared can be used for the removal of ozone from air.

The results of X-ray analysis of fresh Ni/Pd catalysts supported on alumina, carbon and silica are shown in

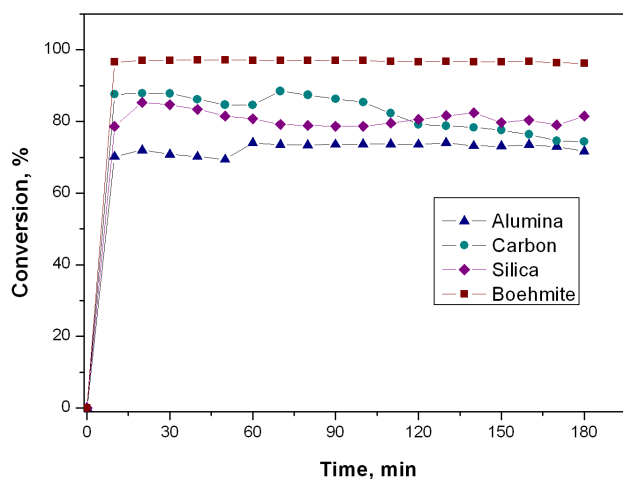


Fig. 1. Ozone conversion as function of ozonation time for the Ni/Pd catalytic samples (the supports are denoted in graph legend).

Fig. 2. The diffractograms are indicative of well pronounced crystal structure of the samples. The peaks at  $43.2^\circ$  and  $62.9^\circ$  in Fig. 2A correspond to nickel oxide. The diffraction features at  $41.5^\circ$ ,  $46.5^\circ$  and  $67.4^\circ$  refer to  $\text{Al}_2\text{O}_3$ . The peaks at  $40.1^\circ$ ,  $46.8^\circ$  and  $68.2^\circ$  show the presence of palladium in the catalytic structure. The peaks at  $37.2^\circ$ ,  $43.3^\circ$  and  $62.9^\circ$  in Fig. 2B correspond to NiO. The diffraction features at  $44.6^\circ$  and  $51.9^\circ$  are determined by nickel presence in the catalytic structure. The peaks at  $40.2^\circ$ ,  $46.7^\circ$  and  $68.2^\circ$  indicate the presence of metal palladium over the carbon. Fig. 2C shows nine features of the catalytic system corresponding to PdO, three peaks referring to palladium and three peaks indicative of NiO.

The ability of the catalyst to decompose ozone depends critically on the noble or transition metal, which must be adequately dispersed in order to provide ozone conversion to molecular oxygen. The morphology and size of the palladium particles present on different supports are studied by high resolution transmission electron microscopy (Fig. 3). There is a clear example in Fig. 3A of a palladium nanoparticle of a size of about 15 nm over an alumina nanocrystal. Fig. 3B shows that the palladium nanoparticles are uniformly dispersed on aggregate clusters of silica nanocrystals. The comparison with 0.17Pd4.7Ni/Al(OH)O catalyst (Fig. 3D) indicates that the metal nanoparticles supported on carbon (Fig. 3C) are equally dispersed on the catalytic surface.

The particle size distributions are elucidated with the application of ImageJ software which is also able to

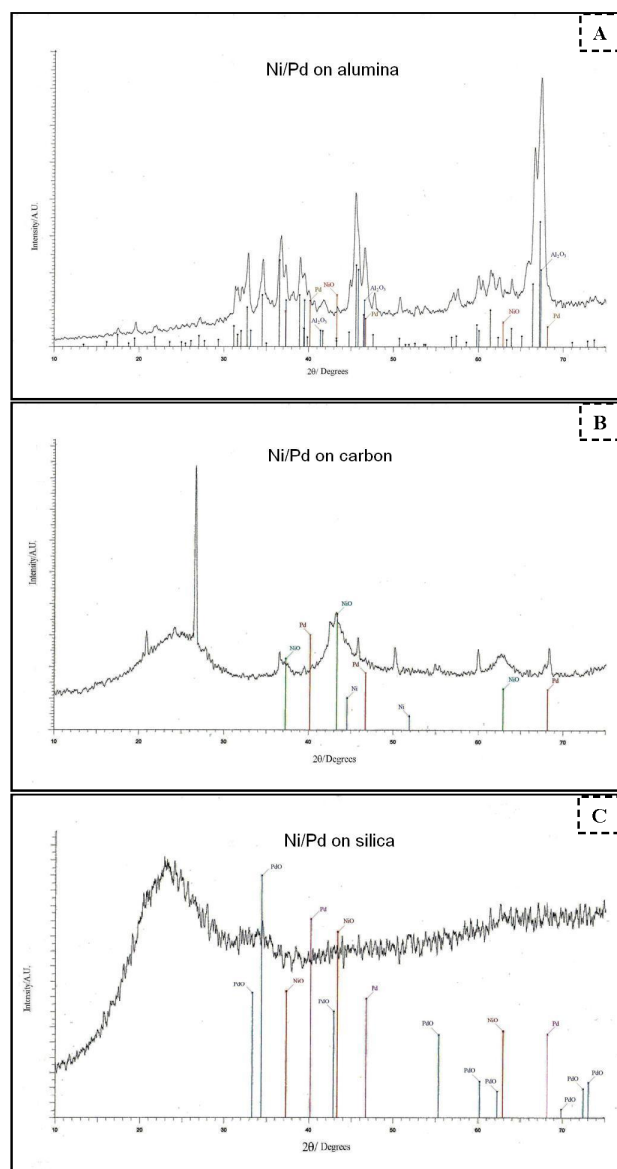


Fig. 2. X-ray diffraction of Ni/Pd catalysts supported on **A** alumina, **B** carbon and **C** silica.

measure the diameter of the particles. In order to calculate the mean particle diameter of 0.17Pd4.7Ni/Carbon catalyst, extra images are taken from several sections of the crystallites. 31 metal particles of the sample are processed aiming statistical treatment of the data. It is found that the mean size refers to 7.1 nm. The distribution of the particles size is illustrated in Fig. 4.

The BET surface areas of the prepared samples are as follows:  $168 \text{ m}^2 \text{ g}^{-1}$  for 0.17Pd4.7Ni/SiO<sub>2</sub>,  $103 \text{ m}^2 \text{ g}^{-1}$  for 0.17Pd4.7Ni/Al(OH)O,  $44 \text{ m}^2 \text{ g}^{-1}$  for 0.17Pd4.7Ni/Al<sub>2</sub>O<sub>3</sub> and  $300 \text{ m}^2 \text{ g}^{-1}$  for 0.17Pd4.7Ni/Carbon.

The EPR spectra of fresh Ni/Pd catalysts recorded

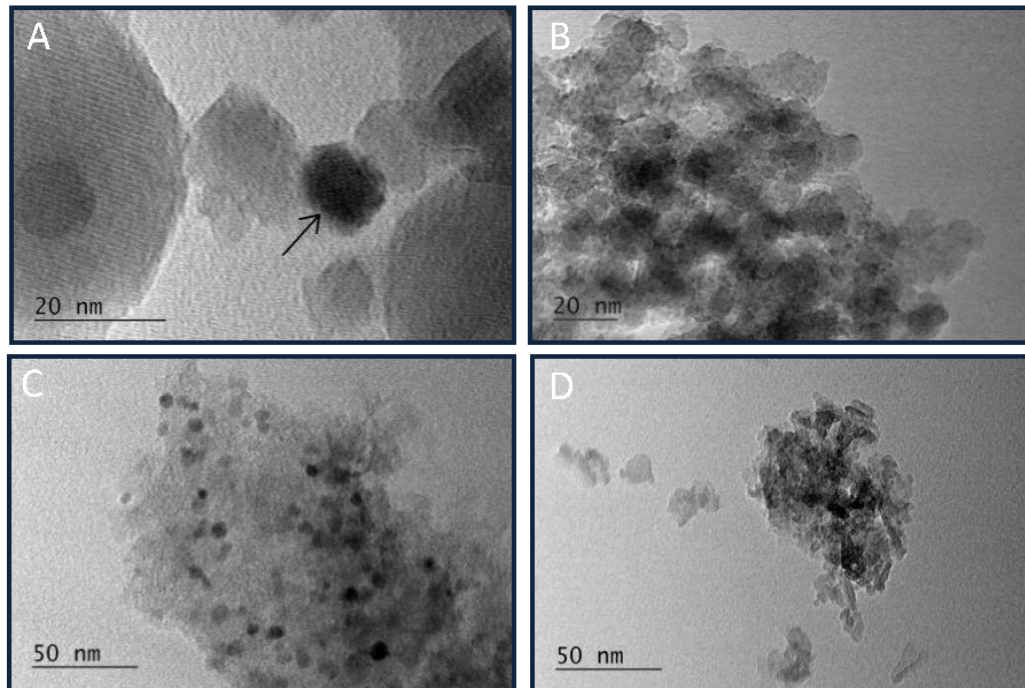


Fig. 3. TEM micrographs of the **A** 0.17Pd4.7Ni/Al<sub>2</sub>O<sub>3</sub>, **B** 0.17Pd4.7Ni/SiO<sub>2</sub>, **C** 0.17Pd4.7Ni/Carbon and **D** 0.17Pd4.7Ni/Al(OH)O catalysts.

at room temperature are presented in Fig. 5. That of 0.17Pd4.7Ni/Carbon (Fig. 5a) includes a broad signal of  $\Delta H = 122$  mT and g factor of 2.28, which is attributed to the ferromagnetic resonance of metallic nickel [14, 15]. Homogeneous magnetization is most probably responsible for the resonance of the separate nickel particles. The g value, which is close to the theoretical value of ca 2.22 [16] is in agreement with the round shape of the particles. The values of g and  $\Delta H$  suggest that the nickel particles on the catalyst surface are finely divided. After ozone treatment (Fig. 6a) the broad EPR signal remains but its line width decreases slightly, while the g value shifts to higher magnetic field. In addition, a new signal appears with g = 2.003. This signal is due to the presence of carbon. It is expected that the interaction of O<sub>3</sub> with electron-excess in the catalytic surface sites leads to the formation of O<sub>3</sub><sup>-</sup> radicals, but that sort of species are not observed.

Fig. 5b shows an EPR spectrum of 0.17Pd4.7Ni/Al(OH)O catalyst. The spectrum consists of two overlapping EPR signals of g values of 2.4 and 2.04, respectively. The signal of g = 2.4 refers most probably to palladium [17]. This means that the oxidation state of palladium can be Pd<sup>3+</sup>, Pd<sup>1+</sup> or Pd<sup>0</sup>. The line width of

the signal cannot be determined because of overlapping EPR lines but the broad spectrum indicates that the signal is due to palladium particles. The second EPR signal of g value of 2.04 is determined by nickel ions presence. The great line width of the EPR spectra suggests dipole-dipole interaction between the cluster ions. The EPR spectrum of ozone treated sample of 0.17Pd4.7Ni/

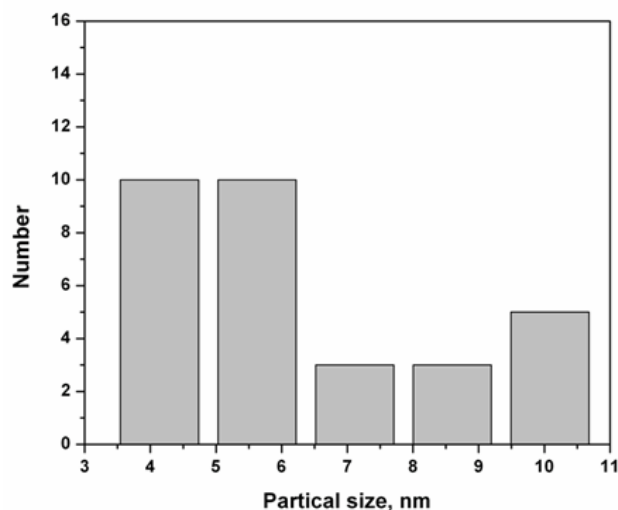


Fig. 4. Particle size distribution histogram of deposited metal acquired from TEM analysis.

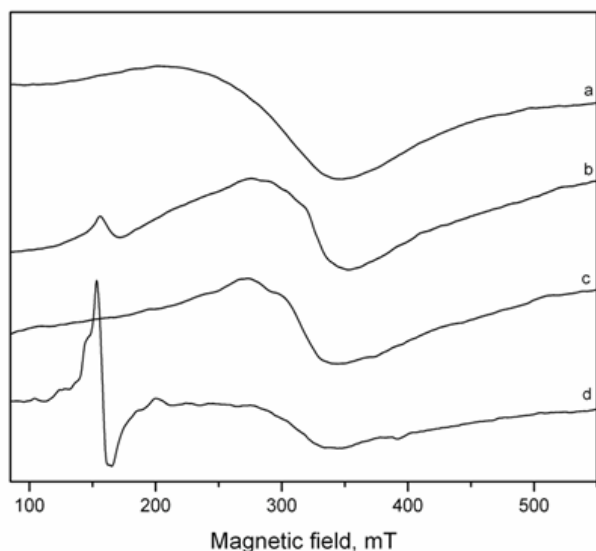


Fig. 5. EPR spectra at room temperature of: a) 0.17Pd4.7Ni/Carbon; b) 0.17Pd4.7Ni/Al(OH)O; c) 0.17Pd4.7Ni/SiO<sub>2</sub>; d) 0.17Pd4.7Ni/Al<sub>2</sub>O<sub>3</sub>.

Al(OH)O catalyst can be seen in Fig. 6b. It is evident that the spectrum is changed. The palladium ions signal dominates the spectrum prior to ozonation, whereas the treatment carried out results in a shift of the effect in respect to the nickel ions. Furthermore, the width of the EPR spectrum decreases. This fact suggests decay of the clusters and presence of isolated Pd<sup>3+</sup> and Ni<sup>2+</sup> ions.

When Ni and Pd are deposited on SiO<sub>2</sub>, the EPR spectrum of the fresh sample (Fig. 5c) is almost the same as that of 0.17Pd4.7Ni/Al(OH)O catalyst (Fig. 5b). Two signals of *g* values of 2.4 and 2.1, referring to palladium and nickel ions, respectively, are observed. The comparison with 0.17Pd4.7Ni/Al(OH)O catalyst after ozone treatment shows that the intensity of the signal arising from palladium particles of ozonated 0.17Pd4.7Ni/SiO<sub>2</sub> sample increases whereas the intensity of the EPR signal of Ni<sup>2+</sup> decreases (Fig. 6c). It is easier to distinguish separate lines after ozone treatment. The line width of the EPR spectrum does not change but the lines are better outlined. This is indication that isolated ions are formed during ozone treatment.

The EPR spectrum of the freshly prepared 0.17Pd4.7Ni/Al<sub>2</sub>O<sub>3</sub> catalyst is shown in Fig. 5d. The spectrum contains a signal of *g* = 2.1 and  $\Delta H = 52$  mT. It is due to Ni<sup>2+</sup> ions in distorted octahedral coordination. After ozonation an axial EPR signal of  $g_{\parallel} = 2.29$  and  $g_{\perp} = 2.07$  is recorded (Fig. 6d). This EPR data is typical

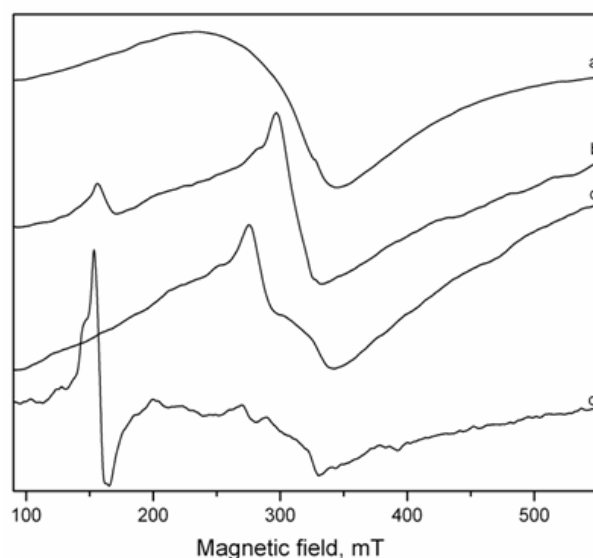


Fig. 6. EPR spectra after ozone treatment: a) 0.17Pd4.7Ni/Carbon; b) 0.17Pd4.7Ni/Al(OH)O; c) 0.17Pd4.7Ni/SiO<sub>2</sub>; d) 0.17Pd4.7Ni/Al<sub>2</sub>O<sub>3</sub> catalysts at room temperature.

of systems containing Ni<sup>2+</sup> ions coordinated by distorted octahedral sites filled with O<sup>2-</sup> or OH<sup>-</sup> ions (Damyanova et al., 1989). In addition, an EPR line of *g* = 2.4 appears. This signal arises from Pd<sup>3+</sup> ions (Tripathi et al., 2005). Hence it can be concluded that diamagnetic Pd<sup>2+</sup> and Pd<sup>4+</sup> transform to paramagnetic Pd<sup>3+</sup> in the course of ozone treatment.

## CONCLUSIONS

It is found that all Ni/Pd catalysts prepared are active in respect to ozone decomposition but the maximum conversion (more than 90 %) is provided by Al(OH)O-supported Ni/Pd system. This result is of importance for the role of nickel and palladium nanoparticles in the catalytic reaction. The distinction in the activities of the catalytic samples prepared on different supports is probably due to the nature of the active sites on every support as well as to the character of interaction between the nickel and palladium nanoparticles with each of the carriers.

The TEM studies evidence the mean size of the metal nanoparticles as well as the influence of the methods of preparation and pre-treatment on the structural and catalytic properties of the samples.

EPR signals of mixed Ni/Pd catalysts are related to species of Pd<sup>3+</sup>, Pd<sup>0</sup>, Ni<sup>0</sup> and Ni<sup>2+</sup>, which have paramagnetic behavior. The existence of oxygen radicals

in ozone treated samples is suggested but so far not observed experimentally.

### Acknowledgements

This work was supported by the ESF under Grant BG051PO001-3.3.06-0050 and FNI under Grant T02 16/12.12.14.

### REFERENCES

1. S. Rakovsky, G. Zaikov, Kinetic and Mechanism of Ozone Reactions with Organic and Polymeric Compounds in Liquid Phase, monograph (2nd ed.), Nova Science Publishers Inc., New York, 2007, 1-340.
2. S. T. Oyama, Chemical and Catalytic Properties of Ozone, Catal. Rev. Sci. Eng., 42, 2000, 279.
3. B. Dhandapani, S. T. Oyama, Gas Phase Ozone Decomposition Catalysts, J. Appl. Catal. B: Environmental, 11, 1997, 129.
4. M. Sugawara, A. Ogata, Effect of Different Combinations of Metal and Zeolite on Ozone-Assisted Catalysis for Toluene Removal, Ozone: Science & Engineering, 33, 2011, 158-163.
5. L. Long, J. Zhao, L. Yang, M. Fu, J. Wu, B. Huang, D. Ye, Room Temperature Catalytic Ozonation of Toluene over  $MnO_2/Al_2O_3$ , Chinese Journal of Catalysis, 32, 2011, 904-916.
6. Martinov, I., S. Tkachenko, V. Demidyuk, G. Egorova, V. Lunin, NiO Addition Influence over Cement-containing Catalysts Activity in Ozone Decomposition, J. Moscow Univ., Ser. 2: Chemistry, 40, 1999, 355-361, (in Russian).
7. X. Li, Q. Zhang, L. Tang, P. Lu, F. Sun, L. Li, Catalytic ozonation of p-chlorobenzoic acid by activated carbon and nickel supported activated carbon prepared from petroleum coke, Journal of Hazardous Materials, 163, 2009, 115-120.
8. D. Pines, D. Reckhow, Solid Phase Catalytic Ozonation Process for the Destruction of a Model Pollutant, Ozone: Science & Engineering, 25, 2010, 25-39.
9. M. Stoyanova, P. Konova, P. Nikolov, A. Naydenov, S. Christoskova, D. Mehandjiev, Alumina-supported nickel oxide for ozone decomposition and catalytic ozonation of CO and VOCs, Chem. Eng. J., 122, 1-2, 2006, 41-46.
10. F. Varela-Gandía, A. Berenguer-Murcia, D. Lozano-Castelló, D. Cazorla-Amorós, D. Sellick, S. Taylor, Total oxidation of naphthalene using palladium nanoparticles supported on BETA, ZSM-5, SAPO-5 and alumina powders, Applied Catalysis B: Environmental, 129, 2013, 98-105.
11. E. Rezaei, J. Soltan, N. Chen, J. Lin, Effect of noble metals on activity of  $MnO_x/\gamma$ -alumina catalyst in catalytic ozonation of toluene, Chemical Engineering Journal, 214, 2013, 219-228.
12. Q. Yu, H. Pan, M. Zhao, Zh. Liu, J. Wang, Y. Chen, M. Gong, Influence of calcination temperature on the performance of Pd-Mn/SiO<sub>2</sub>-Al<sub>2</sub>O<sub>3</sub> catalysts for ozone decomposition, Journal of Hazardous Materials, 172, 2009, 631-634.
13. I. Ivanov, P. Petrova, V. Georgiev, T. Batakliiev, Y. Karakirova, V. Serga, L. Kulikova, A. Eliyas, S. Rakovsky, Comparative Study of Ceria Supported Nano-sized Platinum Catalysts Synthesized by Extractive-Pyrolytic Method for Low-Temperature WGS Reaction, Catalysis Letters, 143, 2013, 942-949.
14. S. Damyanova, A. Spojakina, D. Shopov, Study of low-percentage alumina-supported nickel-molybdenum catalysts by EPR spectroscopy and magnetic measurements, Applied Catalysis, 48, 1989, 177-186.
15. D. Thakur, B. Delmon, The role of group VIII metal promoter in MoS<sub>2</sub> and WS<sub>2</sub> hydrotreating catalysts: I. EPR studies of Co-Mo, Ni-Mo, and Ni-W catalysts, Journal of Catalysis, 91, 2, 1985, 308-317.
16. A. Rubinshtein, F. Lost, A. Slinkin, X-ray diffraction and magnetochemical investigation of Ni-Al<sub>2</sub>O<sub>3</sub> catalysts for the simultaneous hydrogenation and dealkylation of cresols, Izv. Akad. Nauk SSSR, 13, 2, 1964, 229-236.
17. S. Tripathi, R. Kadam, M. Kumar, J. Mittal, S. Misra, EPR investigations on radiation induced chemical transformations in Pd(ClO<sub>4</sub>)<sub>2</sub>/i-PrOH/HClO<sub>4</sub> system from 77 to 300 K, Spectrochimica Acta Part A, 62, 2005, 1107-1113.